

2013-10-03

Modelling gravel beach dynamics with XBeach

Jamal, MH

<http://hdl.handle.net/10026.1/13020>

10.1016/j.coastaleng.2014.03.006

Coastal Engineering

Elsevier

All content in PEARL is protected by copyright law. Author manuscripts are made available in accordance with publisher policies. Please cite only the published version using the details provided on the item record or document. In the absence of an open licence (e.g. Creative Commons), permissions for further reuse of content should be sought from the publisher or author.



Modelling gravel beach dynamics with XBeach

M.H. Jamal^{a,b,*}, D.J. Simmonds^c, V. Magar^d

^a Faculty of Civil Engineering, Universiti Teknologi Malaysia, 81310 Johor Bahru, Johor, Malaysia

^b Coastal and Offshore Engineering Institute (COEI), Universiti Teknologi Malaysia Kuala Lumpur, Jalan Semarak, 54100 Kuala Lumpur, Malaysia

^c School of Marine Science and Technology (Faculty of Science and Technology), University of Plymouth, Drake Circus, PL4 8AA Plymouth, United Kingdom

^d Centro de Investigación Científica y Educación Superior de Ensenada (CICESE), Carretera Ensenada-Tijuana No. 3918, Zona Playitas, C.P. 22860 Ensenada, B.C. México



ARTICLE INFO

Article history:

Received 1 January 2014

Received in revised form 20 March 2014

Accepted 21 March 2014

Available online 17 April 2014

Keywords:

Numerical modelling

Infiltration

Sediment transport

Accretion

Berm

XBeach model

ABSTRACT

Numerical cross-shore profile evolution models have been good at predicting beach erosion during storm conditions, but have difficulty in predicting the accretion of the beach during calm periods. This paper describes the progress made in modifying and applying the public domain XBeach code to the prediction and explanation of the observed behaviour of coarse-grained beaches in the laboratory and the field under accretive conditions. The paper outlines in details the changes made to the original code (version 12), including the introduction of a new morphological module based upon Soulsby's sediment transport equation for waves and currents, and the incorporation of Packwood's infiltration approach in the unsaturated area of the swash region. The competence of this modified model during calm conditions for describing the steepening of the profile, and the growth of the beach berm is demonstrated. Preliminary results on the behaviour of the beach subject to both waves and tides are presented. Good agreement is found between the model simulations and large-scale laboratory measurements, as well as field observations from a composite beach in the UK. The reasons for the model's capabilities are discussed.

© 2014 Elsevier B.V. All rights reserved.

1. Introduction

Despite the focus of much coastal research resting on sandy beaches, coarse-grained beaches are particularly prevalent around the world. Coarse-grained beaches are composed of accumulations of either gravel, or mixed sand and gravel sediments. They are common in mid to high latitude coasts (Carter and Orford, 1993) including the UK. Indeed, approximately, one-third of the beaches in England and Wales are classified as coarse-grained, especially around the south of England (López de San Román-Blanco, 2003). Coarse-grained beaches are an important form of natural coastal defence, protecting significant urban settlements as well as agricultural lands, natural habitats, recreational and environmental assets against wave run-up and storm surge. Coarse-grained beaches are characterized by the presence of a berm in the upper part of the beach. These berms are important sources of sediments during storms and periods of beach erosion (Baldock et al., 2005). Therefore, understanding the morphological behaviour of coarse-grained beaches in response to short-term and long-term forcing is vital for coastal protection. Interest in these environments and their dynamic behaviour in response to wave climate and water level variation has increased in recent years (Bradbury, 2000; Williams et al., 2012).

Sediment size and porosity are very important factors dictating the response of coarse-grained beaches to waves, tides and sea level rise. In general, during swell conditions, the impetus for cross-shore sediment transport over gravel beaches is onshore in the swash region. Gravel is carried upslope as far as the swash extends and deposited to produce a berm in the upper-swash; this also leads to a steepening of the beach face (Bradbury, 1998). This foreshore accretion and increase in beach face slope are against the force of gravity, which requires either the uprush and backwash velocities, or the amounts of sediment transported between uprush and backwash, to be asymmetric (Aagaard and Hughes, 2006). As a result, this increases the beach volume, steepens the beach face and raises the berm crest elevation (Austin, 2005).

It is important to understand that, the balance of processes that govern such behaviour is different to that on sandy beaches, where, for instance, infiltration is negligible. The complex processes associated with the near-shore on gravel beaches, in particular, make it difficult to predict the morphological changes accurately. Several modelling approaches of varying complexity have been reported. These include parametric models (e.g. Powell, 1990) and process-based models (e.g. Clarke et al., 2004; Masselink and Li, 2001; Pedrozo-Acuña et al., 2006).

Time independent parametric models are robust, simpler and easy to apply, but often represent an extreme simplification or ignorance of the key morphological processes, focusing on the representation of profile features by correlation with simple wave, water level

* Corresponding author at: Faculty of Civil Engineering, Universiti Teknologi Malaysia, 81310 Johor Bahru, Johor, Malaysia. Tel.: +60 196582880.
E-mail address: mhidayat@utm.my (M.H. Jamal).

and sediment parameters. Thus, until recently, the most practical, and successful approach to describing coarse beach profiles was provided by the Powell parametric model (Powell, 1990). This empirically derived model is acknowledged to provide a good description of beach profile erosion or the effects of nourishment, based upon a series of intersecting curves and control points.

The aim of this work is to implement a process-based model to study and explain profile changes on gravel beaches over the “short-term”, i.e. over the order of a few hundreds to thousands of waves, under accretive conditions. We investigate the adaptation and use of a public domain numerical model, XBeach (Roelvink et al., 2009; van Thiel de Vries, 2009), based on the non-linear shallow water equations, for capturing the 2D profile dynamics of a gravel beach, through consideration of wave and tidal forcing, building on the work of Jamal et al. (2010, 2012).

2. Dominant processes in gravel beach dynamics

In order to predict the dynamic behaviour of gravel beaches successfully, it is necessary to identify and represent the balance of key processes that control the dynamics of the sediment in the swash zone (Puleo et al., 2000). This is especially true for steeper, coarse-grained beaches where the surf zone is much narrower and closer to the shoreline than on sandy beaches, and where plunging breakers are the dominant wave breaking mode. This creates an environment in which strong pulses of turbulence are generated as the bores collapse close to the shoreline, mobilising even large sediment sizes. The mobilised sediment is then pushed onshore by these bores up the beach face, driven by the swash oscillations (Baldock and Holmes, 1997). These swash oscillations have properties similar to long waves. The generated turbulence dissipates over the short distance, but persists into the swash region with greater intensity in the uprush than in the backwash (Hughes et al., 1997). Another important process in coarse-grained beaches is infiltration, which is more significant on uprush than backwash (Packwood, 1983). Indeed, many studies have stressed the importance of infiltration for sediment transport in the swash region and especially on coarse beaches (e.g. Austin and Masselink, 2006; Horn and Li, 2006; Pedrozo-Acuña et al., 2006, 2007; Turner and Masselink, 1998).

The material property that controls the degree of infiltration is the permeability or hydraulic conductivity of the beach (Masselink and Li, 2001), which can be viewed as altering the bed shear stress (Puleo and Holland, 2001). Permeability tends to be larger in coarse-grained than in sandy beaches (Foote et al., 2002; Heath, 1983). The propensity for onshore transport in the swash is counteracted by the down-slope weight of the sediment, which eventually brings an accreting beach face to a dynamic equilibrium with the incident wave conditions. This balance thus occurs for steeper gradients on coarse, permeable beaches than on sandy beaches. Finally, a number of studies have shown that tides have an important effect on sandy and coarse-grained beach morphology (see, e.g.: Horn and Mason, 1994; Lee et al., 2007; Mason and Coates, 2001; Masselink and Hegge, 1995; Masselink and Short, 1993; Powell, 1990; Raubenheimer et al., 1999; Trim et al., 2002), and their impact on the profile evolution of coarse-grained beaches should be considered.

3. Modelling gravel beach profile change

Serious attempts have been made to model sediment transport in the swash zone of coarse beaches. For instance, Wurjanto and Kobayashi (1993), Van Gent (1994), Clarke et al. (2004) and others have developed different models for simulating flow within and above a porous beach. Although these models allow for infiltration/exfiltration and have been validated for surface elevation and flow

velocities, they have not been used to investigate the effect of this process on sediment transport and beach profile evolution.

Pedrozo-Acuña et al. (2006) reported an experimental and numerical model investigation of cross-shore profile change of a gravel beach. A time dependent morphodynamic model was developed from the Boussinesq model “COULWAVE” (Lynett et al., 2002), which features a moving shoreline boundary to simulate the swash zone. This was coupled to a Meyer-Peter and Müller (1948) sediment transport formulation. They found that if the shear stress and transport efficiency were kept equal during both the uprush and the backwash phases, the numerical predictions were opposite to observations for transport. By adjusting the transport efficiency with swash direction, a better prediction of the observed behaviour was obtained. This ad hoc adjustment of parameters was interpreted as an encapsulation of several processes, including the infiltration of water into the porous beach face and acceleration of flow after wave breaking.

Van Rijn (2010) has reported on the performance of two process-based models, CROSMOR2008 and SHINGLE, as part of the CONSCIENCE project. They found that both models reproduced “swash bars” of the right order of magnitude above the waterline, but that the predicted shapes and positions of the bars did not agree well with laboratory observations. However, both the CROSMOR2008 and SHINGLE models provided good agreement with observations for some large storm events at prototype scale. This indicated some considerable utility in the models, even though the swash processes are not explicitly represented in CROSMOR2008.

Another process-based model recently developed is the open-source numerical modelling system, XBeach (Roelvink et al., 2009; van Thiel de Vries, 2009; see www.xbeach.org). The system comprises a wave and roller module, non-linear shallow water equations (NLSWE) module and morphological module based on Soulsby-van Rijn (SvR) sediment transport equation. The wave module is based upon the Wave Action Balance Equations (WABE) and solves for short waves only on the scale of wave grouping, the long wave being solved through the NLSWE. This model has proven to be a robust and widely used model for morphological studies on sandy beach and dune erosion. The applicability, calibration and validation of the model against laboratory experiments and field observations can be found in Roelvink et al. (2009), van Dongeren et al. (2009), van Thiel de Vries (2009), and McCall et al. (2010). However, the comparisons made in those studies were only for the case of sandy dune erosion. Pender and Karunaratna (2013) have managed to simulate long term behaviour on the sandy Narrabeen beach by combining XBeach with a statistical approach. In this, they switch on a storm and a recovery model according to wave threshold criteria. Ruiz de Alegría-Arzaburu et al. (2010) applied XBeach v18 to a gravel beach in Slapton, UK. They were able to reproduce upper beach erosion during storms, but overestimated the morphological changes. Williams et al. (2012) also found similar results with XBeach, where the model reproduced the erosion of gravel beaches in comparison with the Slapton beach and large-scale experiment (BARDEX). Nevertheless, the model was still unable to produce the observed berm profile. This latest version of XBeach, v19, includes parallel processing to reduce simulation time and a groundwater flow module to simulate infiltration/exfiltration on the beach. The work by Ruiz de Alegría-Arzaburu et al. (2010) and Williams et al. (2012) clearly shows that the latest XBeach model can be used on gravel beaches to predict storm erosion, but its performance has not been tested yet for wave conditions leading to beach accretion, in particular, on a gravel beach. This is the main aim of the current paper.

In this paper, we report on adaptations to XBeach v12, with the aim of extending its applicability to the prediction of gravel beach profile evolution under accretive conditions. The model will also be used to demonstrate the potential for predicting profile evolution over tidal cycles.

4. Application of unmodified XBeach v12 to laboratory data

XBeach v12 comprises Two-Dimensional Horizontal (2DH) formulations for short wave propagation, flow and long wave hydrodynamics, sediment transport and bottom changes for varying waves and flow conditions. The work presented here only considers One-Dimensional Horizontal (1DH) scenario, for cross-shore profile evolution simulations. The morphological changes are calculated using the SvR sediment transport equation. However, the sediment motion is not directly driven by the Lagrangian velocity obtained from the NLSWE. Instead, XBeach uses the Eulerian velocity approximation to drive the sediment movement, obtained by subtracting the Lagrangian velocity from the Stokes drift. This is in order to account for the strong undertow on sandy beaches and dunes. The Eulerian representation produces strong offshore directed velocity profiles on steep slope, which is believed to be more accurate for sandy dune erosion scenarios (McCall et al., 2010; Roelvink et al., 2009).

Since this research concentrates on the cross-shore profile change, the incoming wave direction is set perpendicular to the beach, and this corresponds to the x-axis of our coordinate system. In this case, the Eulerian velocity approximation has the form:

$$u_E = u_L - u_S \quad (1)$$

$$u_S = \frac{E_w}{\rho h c} \quad (2)$$

where, u_L is the Lagrangian velocity obtained from the NLSWE, u_E represents the Eulerian velocity, u_S the Stokes drift, ρ the density of water, h the water depth, E_w the wave energy and c the wave celerity. The SvR formulation is used in the model to calculate the sediment transport. An avalanching process, with separate criteria for critical slopes on wet and dry points, provides a robust solution for slumping of sand during dune erosion.

Some features of the model need further consideration, and therefore, experimental data by López de San Román-Blanco et al. (2006), obtained in the large-scale GWK facilities in Hannover, Germany (2002), is used for this purpose. Fig. 1 shows a schematic of the GWK experiments, where a mobile bed of initial slope of 1:8, and D_{50} of 0.021 m, was laid over an impermeable concrete slab of slope of 1:6. The mobile bed thickness at the water level was 2.0 m, as shown, approximately 275 m from the paddle. The test considered here is the same gravel test as that used by Pedrozo-Acuña et al. (2006), with regular waves of height 0.6 m and period 3.22 s. The profile was measured before and after three consecutive tests of length 500, 1500 and 3000 waves, starting from a graded (flat) beach face.

Figs. 2 and 3 show the results of running the unmodified XBeach v12, with the GWK test after 500 waves. From Fig. 2, it can be seen that the experimental beach accreted and steepened to form a prominent

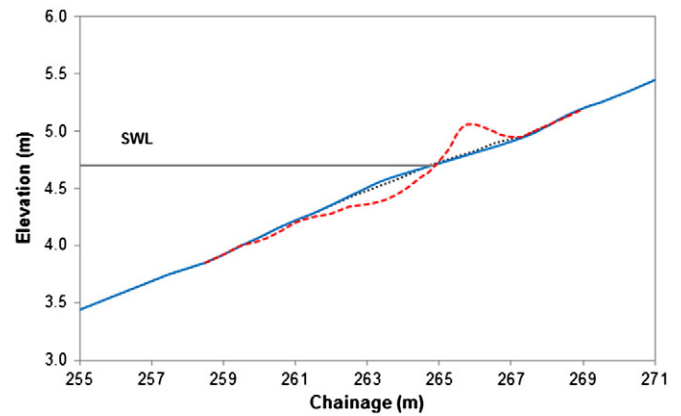


Fig. 2. XBeach v12 comparison with GWK gravel beach test after 500 waves. Original profile (dotted); profile after 500 waves (dashed red); XBeach prediction (solid blue).

swash berm above the still water line (above 4.7 m), and that XBeach fails to capture this behaviour; instead, it predicts net offshore transport. This limitation of XBeach regarding the prediction of berm formation under accretive wave conditions has also been noted by other sources (e.g. Ruiz de Alegría-Arzaburu et al., 2010).

The results shown in Fig. 2 might be anticipated for several reasons. Firstly, the SvR sediment transport equation is being applied beyond its limits of applicability, i.e., for D_{50} larger than 2 mm (Soulsby, 1997). Furthermore, as can be seen in Fig. 3, the Eulerian velocity, which has been used to emphasize the effects of undertow on an eroding sandy dune, is heavily skewed offshore. Finally, in addition to previous discussion, there is no accounting for the infiltration into the porous beach face within the swash region, which acts to reduce the strength of the return flow.

5. A modified XBeach model for coarse sediment

5.1. Lagrangian vs Eulerian velocity representation

Although Silvester and Hsu (1997) found that both the Eulerian and Lagrangian velocity representations give similar values close to the bed, XBeach calculates the Eulerian velocity to represent an enhanced return flow typical of that observed on sandy dune beaches. In contrast, Lara et al. (2002) discussed the differences between water surface envelopes and undertow over impermeable and permeable beds from a laboratory experiment, and showed that the effect of a permeable bed on the undertow is a reduction of the velocity profile close to the bed. Pedrozo-Acuña (2005), and Pedrozo-Acuña et al. (2006) later, analysed the importance of undertow on gravel beaches, using a Boussinesq-type model on a highly permeable gravel beach with a steep foreface and a narrow surf zone. They found that

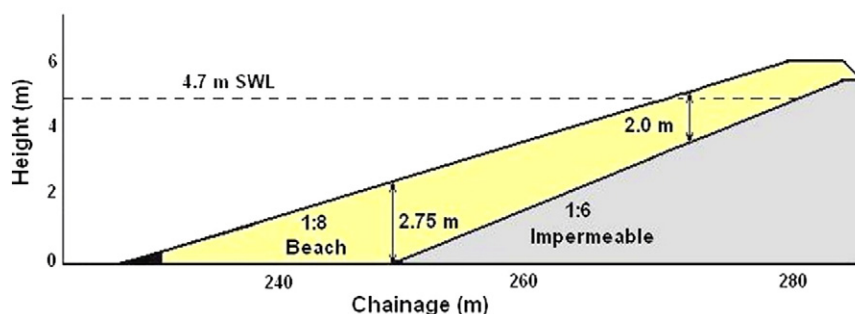


Fig. 1. GWK gravel beach tests schematic. Distance chainage from the wave paddle.

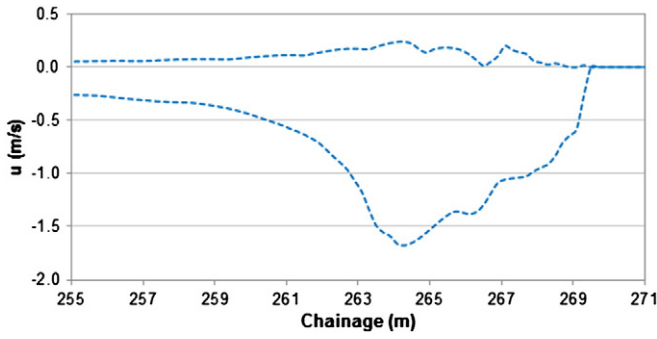


Fig. 3. XBeach v12. Eulerian velocity envelope deduced from NLSWE for 500 waves.

the velocity envelope in the model with undertow and without undertow is very similar on this type of beaches, confirming that on steep gravel beaches undertow or return flow is weak and insignificant. This implies that the roller contribution to return flow and undertow is minimal due to the narrowness of the surf zone. Indeed, Ting and Kirby (1994) showed from their laboratory experiments that undertow is more significant under spilling breakers (gentle slope) than plunging breakers (steep slope).

Therefore, it is concluded that the Lagrangian velocity, calculated from the NLSWE hydrodynamic module could directly be employed in the sediment transport equation in the morphological module. In fact, Tang et al. (2009) and Nam et al. (2009) also used the velocity obtained directly from the NLSWE to drive sediment motion. Tang et al. (2009) illustrated the interactions among waves, currents, and seabed morphology for dam-break over a mobile-bed and evolution of a wave-driven sand dune. Nam et al. (2009) found as well that their model was capable of predicting the nearshore waves, wave-induced current, and sediment transport, when compared to observations from the large-scale sediment transport facility (LSTF) at the Coastal and Hydraulics Laboratory of the U.S. Army Engineer Research and Development Centre in Vicksburg, Mississippi.

The onshore and offshore velocity profile envelopes obtained using the Lagrangian formulation for XBeach v12 are shown in Fig. 4 for the same GWK test case. The envelopes show that the onshore and offshore velocities are now less asymmetric, as anticipated. However, if the same XBeach morphological module used to produce the results shown in Fig. 2 is used to calculate the profile change, the profile change predicted by the new model is now very small (not shown). This is due to the magnitude of the onshore and the offshore velocity is now lower than the threshold velocity for this coarse sediment, compared to the higher offshore velocity magnitude originally obtained with the Eulerian

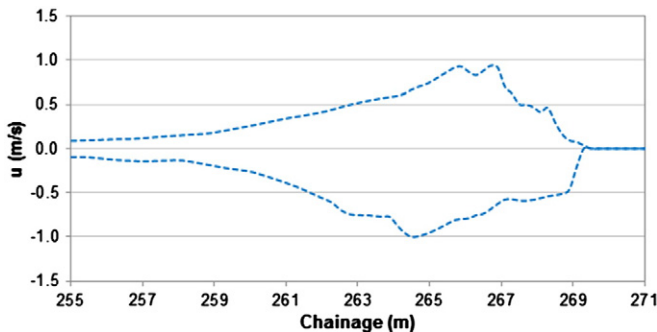


Fig. 4. XBeach v12 velocity envelope from NLSWE for 500 waves: Lagrangian velocity representation.

approximation. Therefore, a new sediment transport formulation needs to be implemented.

5.2. Appropriate coarse sediment transport formulation

The next issue to address was that of finding a more appropriate transport formulation for coarse sediments. For cases where the sediment is large, bed load can be anticipated as the dominant mode of transport in the swash area (e.g. Carter and Orford, 1993; Horn and Mason, 1994; Soulsby, 1997). Thus, we assume a bed load formulation is more suitable, even though some suspension of larger sediment is possible in more energetic conditions. Although there are several possible candidates, the Soulsby's wave and current transport equation (denoted from this point on as SWCTE) was chosen, as this equation is not limited to fine sediments only (Soulsby, 1997; Soulsby and Damgaard, 2005). The sediment transport formulations for the 1DH case are employed; in this formulation, the dimensionless transport rate is $\Phi_x = \max[\Phi_{x1}, \Phi_{x2}]$ when the $\theta_{max} > \theta_{\beta cr}$ and $\Phi_x = 0$ when $\theta_{max} \leq \theta_{\beta cr}$, with:

$$\Phi_{x1} = C_t \theta_m^{1/2} (\theta_m - \theta_{\beta cr}) \quad \text{for } \theta_m > \theta_{\beta cr} \quad (3)$$

$$\Phi_{x2} = C_t (0.9534 + 0.1907 \cos 2\phi) \theta_w^{1/2} \theta_m \quad (4)$$

$$\theta_{max} = \sqrt{(\theta_m + \theta_w \cos \phi)^2 + (\theta_w \sin \phi)^2}. \quad (5)$$

In this formulation, the dimensionless transport rate, Φ_x , depends on: the transport coefficient, C_t ; the dimensionless Shields parameters for the mean shear stress and the wave shear stress, θ_m and θ_w , respectively; ϕ is the angle between the current and the wave ($\phi = 0$ for this case); the critical Shields' parameter with slope, $\theta_{\beta cr}$. It is suggested in Soulsby and Damgaard (2005) that $C_t = 12$ for coarse grains and $C_t = 8$ for fine grains. A more detailed explanation of this sediment transport formulation can be found in Soulsby (1997).

The dimensionless transport is then used to quantify the sediment transport rate, Q_b , as shown in the following equation:

$$Q_b = \Phi_x [g(s-1)D_{50}^3]^{1/2}. \quad (6)$$

Here, s is the relative density and D_{50} is the median grain size. However, a good morphological prediction does not just depend on a suitable sediment transport equation. An accurate description of the hydrodynamics is also very significant. Next, the bed level change is represented as:

$$\frac{\partial z_b}{\partial t} = \frac{1}{(1-n)} \left(\frac{\partial Q_b}{\partial x} \right). \quad (7)$$

Where z_b is the bed level, t is the time and n is porosity.

The profile change for the GWK test with the SWCTE is shown in Fig. 5. With the SWCTE, some bed level changes are now predicted, but the overall movement of sediment is still offshore directed, and no elevated berm is predicted above the waterline. Moreover, between chainages 267 m and 269 m, the simulated profile change is lower than the measured profile, which shows that the run-up reaches higher than expected. However, a more reasonable magnitude for the overall volume change is predicted.

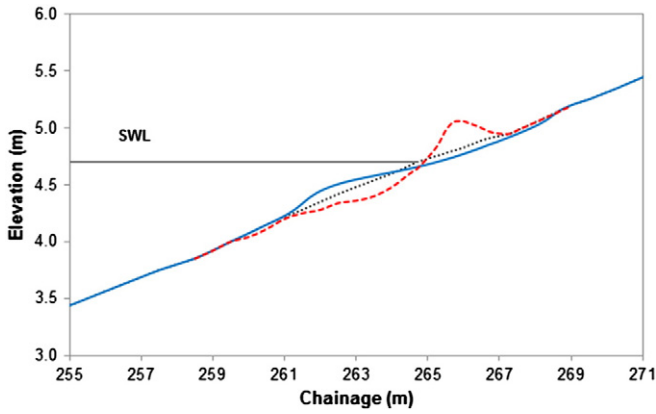


Fig. 5. XBeach with Lagrangian velocity and SWTE. Initial GWK profile (dotted); measured profile (dashed red); XBeach after 500 waves (blue).

In order to produce the observed onshore movement of sediment, clearly that modifications need to be added to the model.

5.3. Implementation of an infiltration model

So far, the adaptations made to XBeach v12 have not improved much of the model predictions for gravel beach evolution under accretive wave conditions. Erosion is predicted against observed accretion. One of the main reasons is that the porosity of coarse sediments has critical effects on profile evolution of gravel and shingle beaches. In particular, the infiltration of the swash lens on the run-up significantly reduces the strength of the backwash.

The implementation of infiltration is adapted from Packwood (1983), which was also used by Stoker and Dodd (2005) and Dodd et al. (2008) to predict beach cusp formation on steep (1:7) coarse beaches, with good results. In brief, an infiltration term q_f is added to the 1DH NLSWE such that:

$$q_f = n \frac{\partial \zeta}{\partial t}. \quad (8)$$

In the unsaturated beach, n is the sediment's porosity and ζ is the depth of free surface inside the porous media (see Fig. 6). However, in the saturated beach the term $q_f = 0$. The depth of infiltration is calculated by the numerical integration of:

$$n \frac{\partial \zeta}{\partial t} = K \left(1 + \frac{h}{\zeta} \right) \quad (9)$$

where, K is the permeability rate or hydraulics conductivity. The 4th order Runge–Kutta method is adopted for the numerical integration of Eq. (4), as suggested by Packwood (1983), and Dodd et al. (2008). On average, the permeability rate K for gravel may vary from 0.001 to 0.1 m/s (Foote et al., 2002; Heath, 1983). However, for mixed sand and gravel, K may be as low as 0.0001 m/s, as the fine sand can fill up the gaps between the gravel (Jackson and Dhir, 1996).

As explained above, the infiltration is assumed to be vertical. At the instant when the unsaturated area is first covered with water at a given location or position, Eq. (9) is singular ($\zeta = 0$). Therefore, an analytical expression for ζ at small t ,

$$\zeta = \frac{K}{2n} \left[1 + \left(1 + \frac{4nh_1}{dtK} \right)^{1/2} \right] dt \quad (10)$$

is needed (Packwood, 1983). In Eq. (10), h_1 is the water depth at the nearest grid point, t is time, and dt is the time step.¹

Rather than trying to attempt to represent the groundwater flow, a more pragmatic approach is taken. The surface water is assumed to be extracted from the surface in the unsaturated area by a certain rate calculated from the above equations which reduce the water depth in that area. This effect is clearly observed during the GWK experiments (López de San Román-Blanco, 2003; Pedrozo-Acuña et al., 2007). Water is extracted from the fluid domain during run-up over the swash area above the still water line (SWL) according to Eq. (3). It should be noted that the mass of water is not currently conserved in the model since recycling of this mass through exfiltration and groundwater flow are not represented. The approach is similar to that implemented by Dodd et al. (2008). The unsaturated area is defined in relation to the SWL; above the SWL, the beach is considered unsaturated and infiltration is allowed. Austin and Masselink (2006) stated that on gravel beaches, the upper beach surface remains unsaturated during the whole tidal cycle hence infiltration occurs throughout the cycle continuously. Horn (2002) also mentioned that the top few centimetres of the beach surface are likely to be partly saturated or unsaturated, allowing for continuous infiltration into the upper beach.

With the infiltration implementation, the 1DH NLSWE model becomes:

$$\frac{\partial \eta}{\partial t} + \frac{\partial hu}{\partial x} = -q_f \quad (11)$$

$$\frac{\partial u}{\partial t} + u \frac{\partial u}{\partial x} - \nu_h \left(\frac{\partial^2 u}{\partial x^2} \right) = -\frac{\tau_{bx}}{\rho h} - g \frac{\partial \eta}{\partial x} + \frac{F_x}{\rho h} - \frac{u q_f}{h} \quad (12)$$

where u is the velocity in the x -direction, ν_h is the horizontal viscosity, t is the time, ρ is the density of water, h is the water depth, τ_{bx} are the bed shear stresses, g is the acceleration of gravity, η is the water level and F_x is the wave-induced stress.

The XBeach v12 model with the three modifications discussed in this section will be called the modified XBeach v12 model from this point onwards.

6. Results using the modified XBeach v12 model

Using the earlier test parameters, the results obtained with the modified XBeach v12 model, shown in Figs. 7 to 11, can be seen correctly moving the sediment onshore and produces a berm on the profile at the top of the gravel beach. It should be noted that Pedrozo-Acuña et al. (2006, 2007) had to change the friction factor, f_c , and the transport coefficient, C_t , on uprush and backwash, to move sediment onshore and approximate the profile development for this test. However, since infiltration has been directly accounted for in the modified XBeach v12 model, the friction factor and transport coefficient can be kept constant throughout the swash cycle. The values used here are $f_c = 0.015$ and $C_t = 12$ as suggested by Soulsby (1997) and Soulsby and Damgaard (2005).

Fig. 7 shows a sensitivity test for three different K values: 0.005, 0.02 and 0.04 m/s. As the backwash motion is weakened by increasing permeability and greater infiltration, its capacity for transporting sediment offshore is more reduced. It was found that as the permeability rate increases, the berm becomes steeper and higher for similar durations of simulation. This occurs because more of the swash lens sinks (more rapidly) into the beach face, resulting in a more asymmetrical, onshore transport. The run-up height is also reduced because of this infiltration

¹ It is worth noting that Dodd et al. (2008) found a misprint in Eq. (6) in Packwood (1983) in relation to this equation, which requires a factor of 1/2 multiplying the right hand side. However, Dodd et al. (2008) also misprinted it in Eq. (A1) as the power of 1/2 is missing at the right hand side.

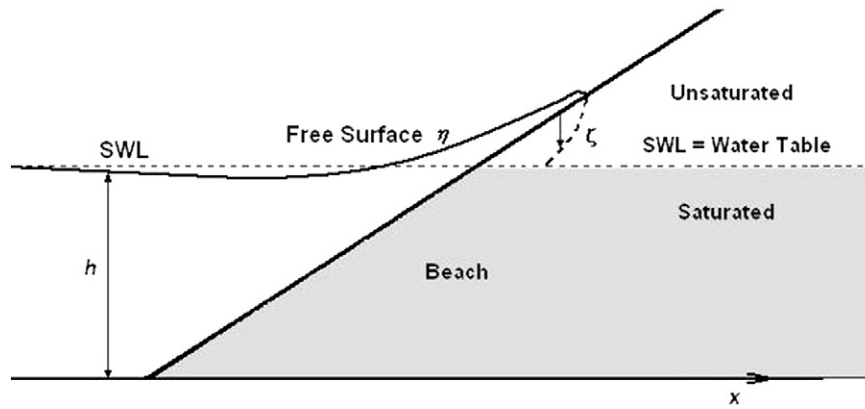


Fig. 6. Schematic of infiltration (after Packwood, 1983).

process. The asymmetry can be clearly seen through the velocity envelopes presented in Fig. 8, for the same three permeability rate values. The velocity envelopes show that infiltration affects the velocity asymmetry, promoting onshore sediment movement for a beach of sufficiently high permeability.

The choice of K used in these simulations to obtain a good prediction is argued to be smaller than might be anticipated. This is because there are still a number of implicit modelling assumptions and limitations:

- At present, the model does not simulate groundwater flow dynamics, which may determine whether the beach is saturated or unsaturated. Thus, no flow inside the beach is considered.
- Above SWL, the beach is always assumed unsaturated. This is not always the case as sometimes the beach can be partially or fully saturated, thus reducing the potential for infiltration.
- No exfiltration is included in the model. This would also affect the net infiltration rate in the dry region.
- Interactions between incoming swash and previous backwash are neglected.
- Air entrapment by the swash lens is neglected. This might reduce the permeability and infiltration rate.
- The assumption of Darcian flow is not entirely appropriate.

Moreover, the permeability of natural beaches is not spatially constant, especially when considering mixed beaches. Notwithstanding these factors, K is assumed to be a constant parameter.

Nevertheless, through judicious choice of parameters, the modified XBeach v12 model is able to reproduce the observed accretion of the beach during this test in the GWK, placing the berm feature quite accurately above the SWL. Brier Skill Scores (BSS) are used to quantify the

agreement between observed and simulated beach profile changes. The BSS is considered as the best measure of how good the prediction of morphological model compares against the measured beach evolution (Sutherland et al., 2004). The prediction of profile change is considered as excellent with the score of between 0.5 and 1.0; good between 0.2 and 0.5; reasonable between 0.1 and 0.2; poor between 0.0 and 0.1; bad for less than 0.0 (Sutherland et al., 2004). Fig. 9 shows a comparison of the simulation using a K value of 0.02 m/s with the GWK test after 500 waves. The asymmetries between onshore and offshore velocities in the hydrodynamic model can be seen to play a significant role in determining the magnitude and direction of sediment transport, and thus in getting the correct cross shore profile evolution. As can be seen from Fig. 9, the modified XBeach v12 model is better than the model by Pedrozo-Acuña et al. (2006) in predicting major profile changes, both in terms of their location and their magnitude. This can be shown from the score of BSS calculated which is 0.86 for the modified XBeach v12 and only 0.08 for the model used by Pedrozo-Acuña et al. (2006). The calculation of BSS here was only around the affected area which is from chainage 257 to 269 m.

Pushing the model further, simulations were executed for 1500 waves (Fig. 10) and with 3000 waves (Fig. 11). Whilst the erosion and deposition locations are still predicted well, the amount of eroded and deposited volume is underpredicted. The BSS for Fig. 10 is 0.78 and BSS for Fig. 11 is 0.67. Although this prediction still considered as excellent, as the beach becomes steeper, the model prediction becomes less accurate. It is believed that this happens because the effect of plunging breakers and associate turbulence becomes more significant in the GWK tests. This will affect the beach profile as discussed in Ting and Kirby (1994, 1995) and Pedrozo-Acuña et al. (2008, 2010). Bore collapse from plunging breakers play an important role in stirring up of sediment from the bed. This physical mechanism was observed in experiments at the GWK for both gravel and mixed beaches.

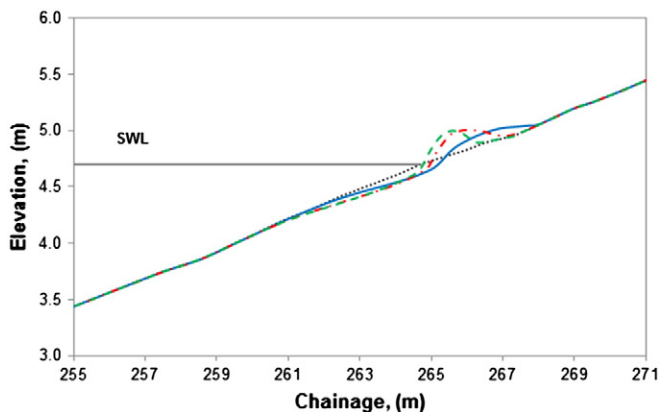


Fig. 7. Modified XBeach v12 model simulation: effect of varying K : Initial beach profile (dot black); $K = 0.005$ m/s (solid blue); $K = 0.02$ m/s (dash-dot red); $K = 0.04$ m/s (dashed green).

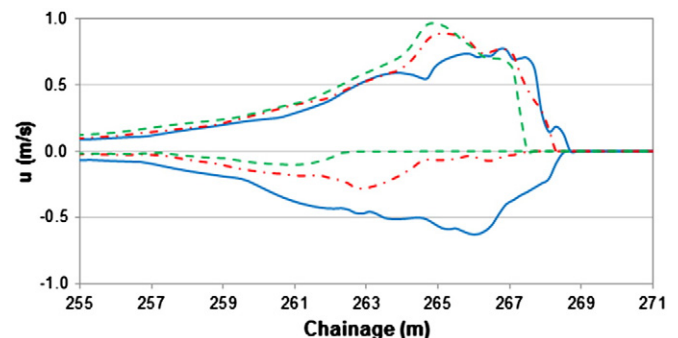


Fig. 8. Sensitivity of velocity envelope to K : $K = 0.005$ m/s (solid blue); $K = 0.02$ m/s (dash-dot red); $K = 0.04$ m/s (dashed green).

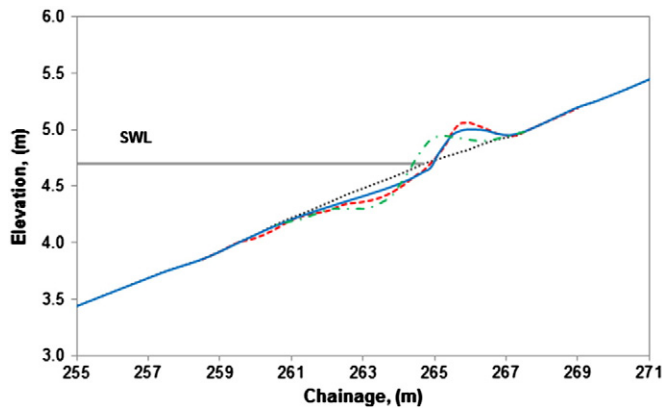


Fig. 9. Comparison of results after 500 waves: initial beach profile (dotted); GWK (dashed red); XBeach model prediction (solid blue); Pedrozo-Acuña et al. (2006) results (dash-dot green).

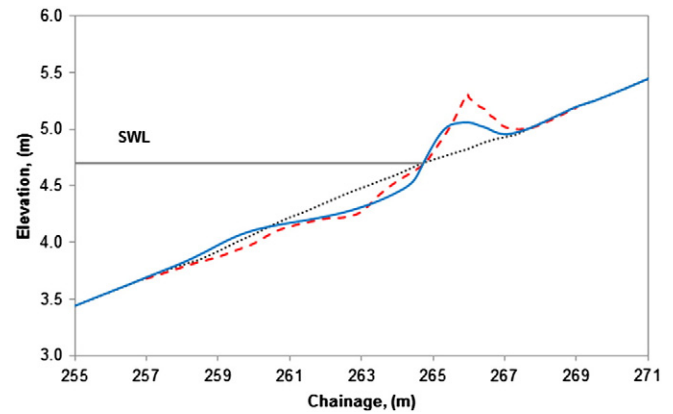


Fig. 11. Result comparison after 3000 waves (measured profile – dashed red; model prediction – solid blue).

Presently, the investigation of the role of turbulence is beyond the scope and complexity of this work. Indeed, the physical representation of plunging breakers is poor when using the NLSWE. The simulations also show that the height of the deposition profile on the upper beach is smaller than the measured one for all three periods. This becomes more evident for longer simulations. It can also be observed that the model attains equilibrium faster than the experiment since a little change is evident in the simulations after 1500 and 3000 waves. This is possibly due to the lack of parameterisations of wave-induced turbulence and associated sediment transport, within the modified XBeach v12 model.

It can also be seen that the model predicts an accumulation of offshore sediment to form a small bar between chainage 258 and 260 after a longer simulation, which is not evident in the GWK experiment. This may be due to the steepness of the beach berm. As the upper beach becomes steeper, less sediment is transported onshore under the same velocity, and hence there is a greater possibility for the sediment in the model to be moved offshore.

7. Simulations with and without tidal excursion for GWK

In this section, the aim is to compare simulations of profile change under stationary and variable water levels due to tidal excursions. The test data from the GWK experiments used are detailed in López de San Román-Blanco (2003). In order to model tidal excursion and investigate the model's capability for predicting profile response in tidal environments (i.e., with non-stationary water level), the approach was

to assume that the water table and the free surface of the external water were closely coupled, by virtue of the relatively high permeability of the sediment. That is, it is assumed that the unsaturated areas on the beach will always follow the level of the surface water elevation. The new simulation uses a simplistic sinusoidal water level variation with a semidiurnal timescale to represent the effective tide with parameters: tidal range 2.5 m; Mean Low Water (MLW) at 3.2 m; Mean High Water (MHW) at 5.7 m relative to the datum corresponding to the GWK test referred to earlier. Again, we use: $K = 0.02$ m/s and friction factor 0.015.

Figs. 12 and 13 show the results for this simulation. This profile has features in common with the non-tidal, accretive profiles shown previously. Fig. 12 shows the first MHW and the first MLW of the tidal cycle. Based on that, the sediment is eroded from the lower beach and carried further up the beach as the surface water rises due to flood, and the sediment is deposited on the upper beach. On the second flood, more sediment is carried into the upper beach, and the size of the berm increases (see Fig. 13). On the second ebb, not much change was found, but still the sediment is carried up the slope. This profile qualitatively agrees with field observations of Horn and Mason (1994), which showed that the sediment transport rate varies throughout the tidal cycle, being greater during flood and lesser during ebb. Therefore, the berm persists on the upper beach.

This preliminary investigation showed that the model was sufficiently stable and capable of predicting anticipated features of profile change associated with a gravel beach under combined wave and tidal forcing. Fig. 14 compares a tidally forced accretion with those predicted

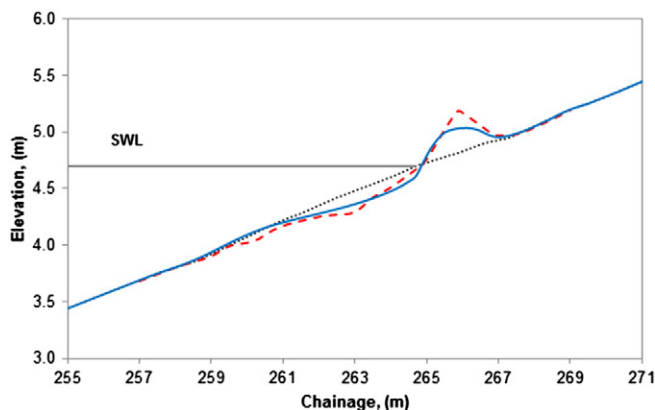


Fig. 10. Result comparison after 1500 waves (measured profile – dashed red; model prediction – solid blue).

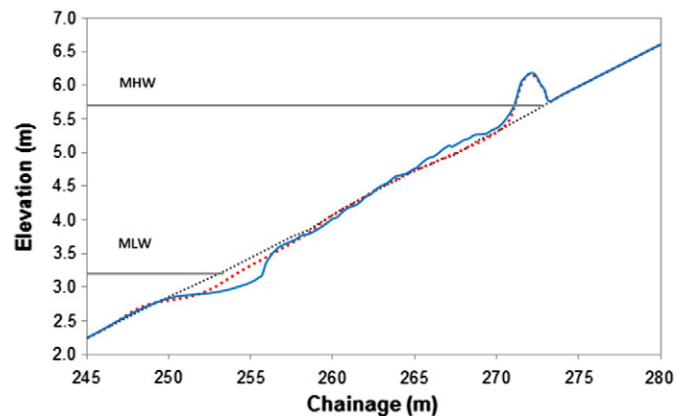


Fig. 12. Tide simulation on gravel beach after first tidal cycle ($K = 0.02$ m/s): initial profile – dotted black; profile after 1st flood – dotted red; profile after 1st ebb – solid blue.

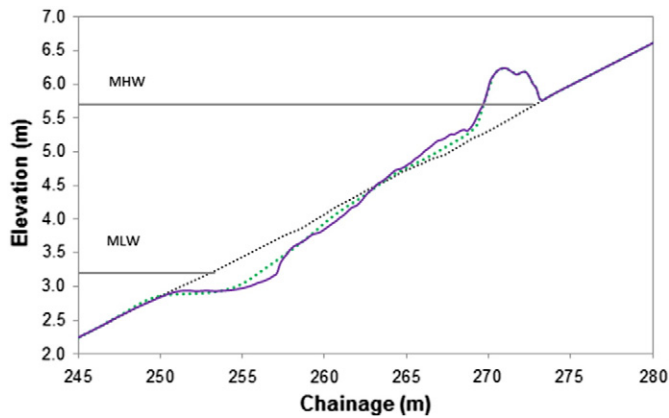


Fig. 13. Tide simulation on gravel beach after two tidal cycle ($K = 0.02$ m/s): initial profile—dotted black; profile after 2nd flood — dotted green; profile after 2nd ebb — solid purple.

under similar beach sediments and wave conditions for constant water level. The figure shows that the affected area of the beach for a day of semidiurnal tide simulation is around 25 m (chainage 248–273 m). As might be expected, the extent of the beach profile change for a stationary mean water level is less, only covering 10 m, between chainage 258 m and 268 m. This result agrees with the result obtained in the laboratory experiments of Trim et al. (2002), which showed that the affected area is wider with tidal fluctuation than under constant water level. The location of the predicted berm was also consistent with observations reported by Powell (1990), i.e. that the berm appears above the intersection of the high water with the beach face. The berm under tidal conditions is found to be bigger in comparison to the berm under non-tidal conditions, in agreement with Trim et al. (2002). Therefore, tides appear to smear berm features over a wider region, with bigger berm size above the flood line, as anticipated. However, these tests demonstrate the ability of the modified XBeach v12 model to simulate many hours of profile change.

8. Simulation of accretion on a coarse meso-tidal beach

Further validation of the modified XBeach v12 model was performed by comparison to beach profile evolution measurements taken from the beach under Hordle Cliff, near Milford-On-Sea, Christchurch Bay, UK

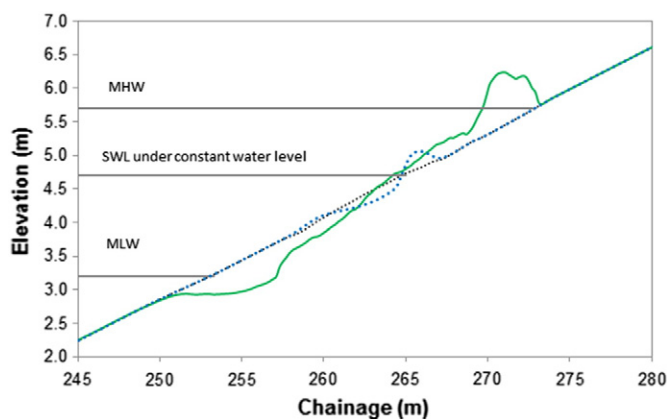


Fig. 14. Gravel beach profile simulation results: simulation of 1 day semidiurnal tide (solid green); simulation of 3000 waves under constant water level (dotted blue); initial beach profile (dotted black).

(Fig. 15). A description of the design of the field experiment is given in Simmonds et al. (2006). The tidal range here varies between 2 m on spring tides to 0.9 m on neap tides. A two month dataset exists of daily beach profile data obtained using a Trimble GPS base station and rover, cross-referenced with local Channel Coastal Observatory benchmarks (www.channelcoast.org). The daily surveys cover 30 shore-normal transects spaced at 10 m intervals, with 1–2 m spacing of points along the transects. Simultaneous measurements of the nearshore wave climate were recorded using a Nortek AWAC deployed approximately 1 km offshore in 7 m depth. Tidal elevation is derived from a tide gauge installed at the field site (type RBR TWRT-2050), cross referenced with an identical gauge located. The wave, tide and beach profile data selected for the data-model comparison were obtained between 28 and 29 October 2007. Over this period the wave approach was shore-normal, minimising contamination of the observations by longshore processes. The tidal excursion and wave data used to drive the 22 h long simulation were based on the field observations averaged over two-hour intervals (see Table 1).

The field site is actually a composite beach with gravel upper beach face and berm, and a lower sandy terrace (Simmonds et al., 2006). The sediment size used in the simulation is based on the measured $D_{50} = 7.2$ mm around the mean sea level (MSL). For this comparison, a smaller permeability of 0.005 m/s was used. This value was chosen to reflect the lower permeability caused by the presence of finer sediment. A friction factor of 0.02 was used and transport coefficient of 12 which Soulsby and Damgaard (2005) suggest is suitable for coarse material. The comparison is not expected to capture the dynamics of the lower sandy terrace, and hence focuses on the upper beach and berm.

Fig. 16 shows comparisons of the initially observed beach profile with the profile observed after two tides and the model simulation. The initial profile used in the model simulation is the observed profile on 28 October 2007. This blind, first application of the model demonstrates that it is able to predict relatively well the major features of the profile change over one day. The value of BSS here is 0.45 which can be classified as good. The location of the berm above the flood tide level agrees well with the measured berm development, although the magnitude of accretion here is less. Between the high water and low water levels (marked “MLW” and “MHW”), the model predicts more erosion than measured in the field and the model deposits more sediment offshore, below the low water level. This may be due to the effect of bore collapse and wave breaking, which is not considered in the current work. It is believed that as the beach becomes steeper, the effect of plunging waves and associated turbulence over the beach face increases. Hence, this will affect the beach profile as discussed in Ting and Kirby (1994) and Pedrozo-Acuña et al. (2008). This bore collapse from plunging breakers play an important role in stirring up of sediment from the bed. This physical mechanism was observed in Pedrozo-Acuña et al. (2006, 2007, 2008) during the experiments for gravel and mixed beaches at the GWK. The model cannot yet cope with multiple grain fractions, which is evident in the poor representation of the lower sandy terrace.

9. Conclusion

The modified XBeach v12 model has been shown capable of predicting 1DH gravel beach dynamics for a sequence of laboratory tests during which a beach was observed to accrete, forming a swash berm above the SWL. This was achieved through modifying the original XBeach v12 as follows: using the Lagrangian velocity calculated directly from the NLSWE to drive the sediment transport module; changing the transport formulation to be more appropriate for coarse sediment; allowing the infiltration of swash run-up into the beach face.

Of the three changes, the last has the most noticeable effect on the direction of sediment transport and prediction of the berm formation



Fig. 15. Coarse-grained beach (Milford-On-Sea, Christchurch Bay, UK).

in the upper beach. Moreover, the modified XBeach v12 model succeeds in predicting the correct amount of transport. It is suggested that the short wave action has been transferred into the long wave motions by the model, generating a correct estimate of their combined effect in the swash zone.

The robustness of the modified XBeach v12 model also permits long simulations, of the order of days, to be performed. It was thus possible to investigate the effect of tidal excursion on processes across a coarse beach profile. Tides are known to affect the water table levels within the beach, and this can affect infiltration and the subtle switch between beach steepening (accretion) and flattening (erosion). Here, the modified XBeach v12 model was evaluated for its stability in simulating coarse beach profile dynamics over several idealised tidal cycles. This was compared with a similar length simulation with a stationary mean water level. The initial beach profile and wave conditions used were taken from those of an experiment in the GWK. All the other model parameters such as permeability rate, friction factor and porosity were kept constant between the simulations. The model predictions show behaviour consistent with observations from laboratory experiments (Trim et al., 2002) and field experiments (Horn and Mason, 1994; Powell, 1990) in terms of the affected area, the rate of sediment transport (during flood and ebb) and the berm location and larger size under tidal conditions. An initial favourable comparison was also made between the model simulation and field observations from a composite beach at Milford-on-Sea, using the measured parameters.

In conclusion, it can be seen that this modified XBeach v12 model, which is based on the system developed for simulating sandy dune erosion, promises to be a useful system for investigating other environments, including accretion and erosion on gravel beaches. Work is ongoing to validate this model for a wider selection of cases, and to further investigate profile evolution of gravel beaches and other environments. It is also intended to show that this model can be used to simulate both erosion and accretion on gravel beaches.

Acknowledgement

The large-scale tests in the Large Wave Channel (GWK) of the Coastal Research Centre (FZK) were supported by the European Community under the Access to Research Infrastructures action of the Human Potential Programme (contract HPRI-CT-1999-00101). The authors would also like to acknowledge the support of the European Commission through the project “Innovative Technologies for safer European coasts in a changing climate” (THESEUS), Contract 244104, FP7.2009-1.

Mohamad H. Jamal is grateful to the Malaysian Government and Universiti Teknologi Malaysia for sponsorship of his research studies at the University of Plymouth, United Kingdom. We finally wish to express our gratitude to the XBeach development team and its funders for maintaining the code in the public domain (www.xbeach.org) and for our discussions with Robert McCall.

Table 1
Tidal excursion and wave observations, 28–29th October 2007.

Time (h)	Tidal excursion (Ordnance datum, m)	Wave height (m)	Wave period (s)	Time (h)	Tidal excursion (Ordnance Datum, m)	Wave height (m)	Wave period (s)
0–2	−0.3 → 0.5	1.34	7.06	12–14	−0.7 → 0.5	0.46	8.22
2–4	0.5 → 0.93	1.41	6.68	14–16	0.5 → 0.86	0.48	7.38
4–6	0.93 → 0.79	1.31	6.61	16–18	0.86 → 0.96	0.52	7.06
6–8	0.79 → 0.72	1.04	7.67	18–20	0.96 → 0.8	0.56	6.79
8–10	0.72 → −0.39	0.92	8.14	20–22	0.8 → −0.12	0.51	7.60
10–12	−0.39 → −0.7	0.64	9.09				

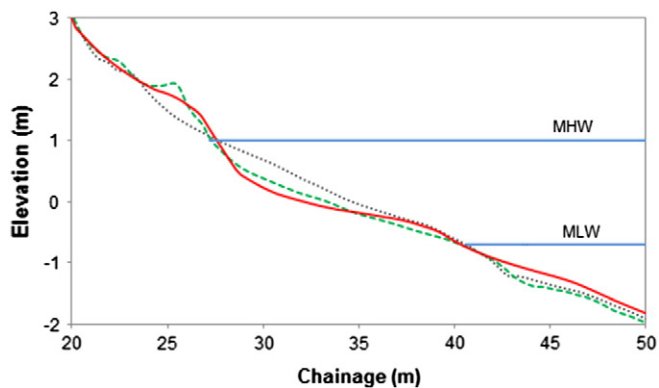


Fig. 16. Milford on Sea beach profile simulation: initial beach profile (dotted black); simulated profile (solid red); measured profile (dashed green).

References

- Aggaard, T., Hughes, M.G., 2006. Sediment suspension and turbulence in the swash zone of dissipative beaches. *Mar. Geol.* 228 (1–4), 117–135.
- Austin, M.J., 2005. Swash, Groundwater and Sediment Transport Processes on a Gravel Beach. (PhD thesis) Loughborough University, U.K.
- Austin, M.J., Masselink, G., 2006. Swash–groundwater interaction on a steep gravel beach. *Cont. Shelf Res.* 26 (20), 2503–2519.
- Baldock, T.E., Holmes, P., 1997. Swash hydrodynamics on a steep beach. *Proceedings Coastal Dynamics '97*, ASCE, Plymouth, UK, pp. 784–793.
- Baldock, T.E., Hughes, M.G., Day, K., Louys, J., 2005. Swash overtopping and sediment overwash on a truncated beach. *Coast. Eng.* 52 (7), 633–645.
- Bradbury, A.P., 1998. Response of Shingle Barrier Beaches to Extreme Hydrodynamic Conditions. (PhD thesis) University of Southampton, U.K.
- Bradbury, A.P., 2000. Predicting breaching of shingle barrier beaches—recent advances to aid beach management. 35th MAFF (DEFRA) Conf. of River and Coastal Engineers.
- Carter, R.W.G., Orford, J.D., 1993. The morphodynamics of coarse clastic beaches and barriers: a short and long-term perspective. *J. Coast. Res.* 15, 158–179.
- Clarke, S., Dodd, N., Damgaard, J., 2004. Modeling flow in and above a porous beach. *J. Waterw. Port Coast. Ocean Eng.* 130 (5), 223–233.
- Dodd, N., Stoker, A.M., Calvete, D., Sriariyawat, A., 2008. On beach cusp formation. *J. Fluid Mech.* 597, 145–169.
- Foot, M., Horn, D., Li, L., 2002. Measuring swash zone hydrodynamics and morphodynamic change — a high-resolution laboratory system using digital video. *J. Coast. Res.* 18, 300–316.
- Heath, R.C., 1983. Basic ground-water hydrology. US Geological Survey Water Supply, paper 2220.
- Horn, D.P., 2002. Beach groundwater dynamics. *Geomorphology* 48 (1–3), 121–146.
- Horn, D., Li, L., 2006. Measurement and modelling of gravel beach groundwater response to wave run-up: effects on beach profile changes. *J. Coast. Res.* 22 (5), 1241–1249.
- Horn, D.P., Mason, T., 1994. Swash zone sediment transport mode. *Mar. Geol.* 120 (3–4), 309–325.
- Hughes, M., Masselink, G., Hanslow, D., Mitchell, D., 1997. Toward a better understanding of swash zone sediment transport. *Proceedings of Coastal Dynamics '97*, ASCE, Plymouth, UK, pp. 804–813.
- Jackson, N., Dhir, R.K., 1996. *Civil Engineering Material*. MacMillan Press Ltd., Hampshire, U.K.
- Jamal, M.H., Simmonds, D.J., Magar, V., Pan, S., 2010. Modelling infiltration on gravel beaches with an XBeach variant. *Proceedings of 32nd International Conference on Coastal Engineering*, No. 32(2010), Shanghai, China, Paper No. 156, pp. 1–11.
- Jamal, M.H., Simmonds, D.J., Magar, V., 2012. Gravel beach profile evolution in wave and tidal environment. *Proceedings of 33rd International Conference on Coastal Engineering*, Santander, Spain, Paper No. 491, pp. 1–10.
- Lara, J.L., Losada, I.J., Cowen, E.A., 2002. Large-scale turbulence structures over an immobile gravel-bed inside the surf zone. *Proceedings of 28th International Conference on Coastal Engineering*, Cardiff, UK, pp. 1050–1061.
- Lee, K.H., Mizutani, N., Hur, D.S., Kamiya, A., 2007. The effect of groundwater on topographic changes in a gravel beach. *Ocean Eng.* 34 (3–4), 605–615.
- López de San Román-Blanco, B., 2003. Dynamics of Gravel and Mixed, Sand and Gravel Beaches. (PhD thesis) Imperial College, University of London, London, U.K.
- López de San Román-Blanco, B., Coates, T.T., Holmes, P., Chadwick, A.J., Bradbury, A.P., Baldock, T.E., Pedrozo-Acuña, A., Lawrence, J., Grüne, J., 2006. Large scale experiments on gravel and mixed beaches: experimental procedure, data documentation and initial results. *Coast. Eng.* 53 (4), 349–362.
- Lynett, P.J., Wu, T.R., Liu, P.L.F., 2002. Modelling wave runup with depth-integrated equations. *Coast. Eng.* 46 (2), 89–107.
- Mason, T., Coates, T.T., 2001. Sediment transport processes on mixed beaches: a review for shoreline management. *J. Coast. Res.* 17 (3), 645–657.
- Masselink, G., Hegge, B., 1995. Morphodynamics of meso- and macrotidal beaches: examples from central Queensland, Australia. *Mar. Geol.* 129 (1–2), 1–23.
- Masselink, G., Li, L., 2001. The role of swash infiltration in determining the beach face gradient: a numerical study. *Mar. Geol.* 176 (1–4), 139–156.
- Masselink, G., Short, A.D., 1993. The effect of tide ranges on beach morphodynamics and morphology: a conceptual beach model. *J. Coast. Res.* 9 (3), 785–800.
- McCall, R.T., Thiel, Van, de Vries, J.S.M., Plant, N.G., Van Dongeren, A.R., Roelvink, J.A., Thompson, D.M., Reniers, A.J.H.M., 2010. Two-dimensional time dependent hurricane overwash and erosion modeling at Santa Rosa Island. *Coast. Eng.* 57 (7), 668–683.
- Meyer-Peter, E., Müller, R., 1948. Formulas for bed load transport. 2nd Congress of the Int. Association of Hydraulics Structures Res., Stockholm, Sweden.
- Nam, P.T., Larson, M., Hanson, H., Hoan, L.X., 2009. A numerical model of nearshore waves, currents, and sediment transport. *Coast. Eng.* 56 (11–12), 1084–1096.
- Packwood, A.R., 1983. The influence of beach porosity on wave uprush and backwash. *Coast. Eng.* 7 (1), 29–40.
- Pedrozo-Acuña, A., 2005. Concerning Swash on Steep Beaches. (PhD thesis) University of Plymouth, U.K.
- Pedrozo-Acuña, A., Simmonds, D.J., Otta, A.K., Chadwick, A.J., 2006. On the cross-shore profile change of gravel beaches. *Coast. Eng.* 53 (4), 335–347.
- Pedrozo-Acuña, A., Simmonds, D.J., Chadwick, A.J., Silva, R., 2007. A numerical–empirical approach for evaluating morphodynamic processes on gravel and mixed sand–gravel beaches. *Mar. Geol.* 241 (1–4), 1–18.
- Pedrozo-Acuña, A., Simmonds, D.J., Reeve, D.E., 2008. Wave-impact characteristics of plunging breakers acting on gravel beaches. *Mar. Geol.* 253 (1–2), 26–35.
- Pedrozo-Acuña, A., Torres-Freyermuth, A., Zou, Q., Hsu, T.J., Reeve, D.E., 2010. Diagnostic investigation of impulsive pressures induced by plunging breakers impinging on gravel beaches. *Coast. Eng.* 57 (3), 252–266.
- Pender, D., Karunarathna, H., 2013. A statistical-process based approach for modelling beach profile variability. *Coast. Eng.* 81, 19–29.
- Powell, K.A., 1990. Predicting Short Term Profile response for shingle beaches. Report SR 219. HR Wallingford, Oxfordshire, U.K.
- Puleo, J.A., Holland, K.T., 2001. Estimating swash zone friction coefficients on sandy beach. *Coast. Eng.* 43 (1), 25–40.
- Puleo, J.A., Beach, R.A., Holman, R.A., Allen, J.S., 2000. Swash zone sediment suspension and transport and the importance of bore-generated turbulence. *J. Geophys. Res.* 105 (C7), 17021–17044.
- Raubenheimer, B., Guza, R.T., Elgar, S., 1999. Tidal water table fluctuations in a sandy ocean beach. *Water Resour. Res.* 35 (8), 2313–2320.
- Roelvink, D., Reniers, A., van Dongeren, A., van Thiel de Vries, J., McCall, R., Lescinski, J., 2009. Modelling storm impacts on beaches, dunes and barrier islands. *Coast. Eng.* 56 (11–12), 1133–1152.
- Ruiz de Alegria-Arzaburu, A., Williams, J., Masselink, G., 2010. Application of XBeach to model storm response on a macrotidal gravel barrier. *Proceedings of 32nd International Conference on Coastal Engineering*, Shanghai, China.
- Silvester, R., Hsu, J.R.C., 1997. Coastal stabilization. *Advanced Series on Ocean Engineering*, vol. 14. World Scientific Publishing Co. Pte. Ltd, Singapore.
- Simmonds, D., Davidson, M., Reeve, D., Chadwick, A., Dong, P., Spivack, M., Kizhisseri, A., Karunarathna, H., Wu, X., 2006. A risk based framework for predicting long-term beach evolution. *Proceedings of the 30th International Conference on Coastal Engineering*.
- Soulsby, R.L., 1997. *Dynamics of marine sands*. Thomas Telford/HR Wallingford, London, U.K.
- Soulsby, R.L., Damgaard, J.S., 2005. Bedload sediment transport in coastal waters. *Coast. Eng.* 52 (8), 673–689.
- Stoker, A., Dodd, N., 2005. Evolution of beach cusp. *Proceedings of Coastal Dynamics '05*, ASCE, Barcelona, Spain (11 pp.).
- Sutherland, J., Peet, A.H., Soulsby, R.L., 2004. Evaluating the performance of morphological models. *Coast. Eng.* 51 (8–9), 917–939.
- Tang, H.S., Keen, T.R., Khanbilvardi, R., 2009. A model-coupling framework for nearshore waves, currents, sediment transport and seabed morphology. *Commun. Nonlinear Sci. Numer. Simul.* 14, 2935–2957.
- Ting, F.C.K., Kirby, J.T., 1994. Observation of undertow and turbulence in a laboratory surf zone. *Coast. Eng.* 24 (1–2), 51–80.
- Ting, F.C.K., Kirby, J.T., 1995. Dynamics of surf-zone turbulence in a strong plunging breaker. *Coast. Eng.* 24 (3–4), 177–204.
- Trim, L.K., She, K., Pope, D.J., 2002. Tidal effects on cross-shore sediment transport on a shingle beach. *J. Coast. Res.* 18, 708–715.
- Turner, I.L., Masselink, G., 1998. Swash infiltration–exfiltration and sediment transport. *J. Geophys. Res.* 103 (C13), 30813–30824.
- Van Dongeren, A., Bolle, A., Voudoukas, M.I., Plomaritis, T., Eftimova, P., Williams, J., Armario, C., Idier, D., Van Geer, P., Van Thiel de Vries, J., Haerens, P., Taborda, R., Benavente, J., Trifonova, E., Ciavola, P., Balouin, Y., Roelvink, D., 2009. MICORE: Dune erosion and overwash model validation with data from nine European field sites. *Proceedings of Coastal Dynamics '09*, Tokyo, Japan, paper no. 82, pp. 1–15.
- Van Gent, M.R.A., 1994. The modelling of wave action on and in coastal structures. *Coast. Eng.* 22 (3–4), 311–339.
- Van Rijn, L.C., 2010. Modelling erosion of gravel/shingle beaches and barriers. EU FP6 project: Concepts and Science for Coastal Erosion Management (CONSCIENCE), report D13b (available at: www.conscience-eu.net).
- Van Thiel de Vries, J.S.M., 2009. Dune erosion during storm surges. (PhD thesis) Delft, Netherlands.
- Williams, J., Ruiz de Alegria-Arzaburu, A., McCall, R.T., Van Dongeren, A., 2012. Modelling gravel barrier profile response to combined waves and tides using XBeach: laboratory and field results. *Coast. Eng.* 63, 62–80.
- Wurjanto, A., Kobayashi, N., 1993. Irregular wave reflection and runup on permeable slope. *J. Waterw. Port Coast. Ocean Eng.* 119 (5), 537–557.